ORGANIC CHEMISTRY FRONTIERS

RESEARCH ARTICLE

View Article Online
View Journal | View Issue

Cite this: *Org. Chem. Front.*, 2026, **13**, 794

Electronic structure origins of radical character in triangular fused acenes: sextet stabilization *vs.* antiaromaticity release

José Aarón Rodríguez-Jiménez, †[a,b] Jan Patrick Calupitan *†[a,c,d] and David Casanova *[a,e]

Received 24th September 2025,
Accepted 26th November 2025

DOI: 10.1039/d5qo01343g

rsc.li/frontiers-organic

Open-shell hydrocarbons are of great interest in molecular materials, yet their electronic structures remain challenging to describe. Here we investigate triangular acenes, formed by fusing three identical linear acenes through cyclobutadiene linkers into a threefold symmetric framework. Using density functional and multi-configurational methods, we show that triangular acenes display a stronger radical character than their linear counterparts, which increases with molecular size. Analysis of singlet–triplet gaps, unpaired electron numbers, and NICS(1) aromaticity indices reveals that this behavior arises from two cooperative effects: Clar's sextet stabilization and the release of cyclobutadiene antiaromaticity. Fractional occupation densities further indicate a redistribution of unpaired electrons from cyclobutadiene units in smaller molecules to the acene cores in larger systems. These results establish triangular acenes as a distinct class of multiradicaloid hydrocarbons, offering new insights for the design of open-shell π-conjugated materials.

Introduction

Fuelled by advances in synthesis and characterisation techniques, a renewed interest in open-shell[1–3] organic compounds and materials in the past decade has opened new directions in the fields of opto-electronics,[4–7] spintronics,[7,8] and chemical synthesis.[9–11] Both bulk solution synthesis[12,13] and surface-supported[14,15] methods rendered access to probe the electronic, magnetic, and chemical properties of carbon-based molecules with unpaired electrons (*i.e.* radicals) or open-shell character (*i.e.* radicaloids). Typical examples include triphenylmethyl,[4,5] nitroxide,[10] acenes,[16–31] triangulenes,[32–39] Clar's goblet,[40–42] and their derivatives.

The study and application of radical and radicaloid species pose significant challenges, both experimentally and computationally. Experimentally, radicals suffer from stability issues due to the presence of unpaired electrons, while radicaloids are often destabilized by their intrinsically small electronic bandgaps. Computationally, the intricate electronic structure of open-shell molecules severely limits the accuracy of theoretical approaches. Density functional theory (DFT) has proven highly successful in describing a wide variety of molecular systems and properties,[43] offering an excellent balance between accuracy and computational cost. However, the reliable treatment of low-spin states with unpaired electrons, commonly associated with the strong electron correlation problem, remains a major unresolved challenge within DFT. In contrast, multiconfigurational wavefunction methods can naturally capture strong correlation effects, but their steep computational cost significantly restricts the size and complexity of the systems that can be feasibly studied.

Among organic compounds with open-shell character, linear acenes (A*n*, see Fig. 1) represent one of the most extensively studied families. Their radical character is known to increase systematically with molecular length, making them paradigmatic systems for investigating the emergence of strong correlation in π-conjugated frameworks. Beyond their fundamental relevance, acenes have attracted wide attention due to their distinctive electronic and photophysical properties,[16–21] as well as their role as benchmark systems for testing and developing novel theoretical approaches.[21–24] Notably, the radicaloid nature of acenes larger than pentacene have been predicted[21–23] and their increasing open-shell character have been confirmed by experimental approaches.[16–18] While the presence of unpaired electrons in tridecacene have been experimentally confirmed recently,[25] several

[a]*Donostia International Physics Center (DIPC), 20018 Donostia, Euskadi, Spain. E-mail: david.casanova@dipc.org*
[b]*Polimero eta Material Aurreratuak: Fisika, Kimika eta Teknologia, Kimika Fakultatea, Euskal Herriko Unibertsitatea (UPV/EHU), 20018 Donostia, Euskadi, Spain*
[c]*Centro de Física de Materiales (CFM-MPC), CSIC-UPV/EHU, 20018 San Sebastián, Spain*
[d]*Sorbonne Université, CNRS, Institut Parisien de Chimie Moléculaire, IPCM, F-75005 Paris, France. E-mail: jan.calupitan@sorbonne-universite.fr*
[e]*IKERBASQUE, Basque Foundation for Science, 48009 Bilbao, Euskadi, Spain*
†These authors contributed equally.

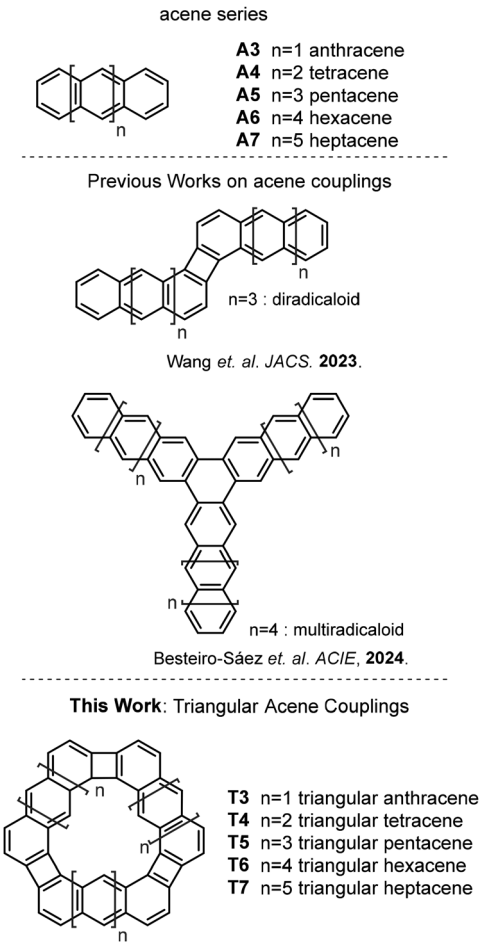

Fig. 1 (Top) Structures and naming conventions of acene series. (Middle) Previous works showing open-shell character for acenes connected *via* cyclobutadiene moiety. (Bottom) Triangular acenes investigated in this work.

works suggest that coupling acenes, even small units, could also induce an open-shell character according to their coupling motifs.[26–29] To illustrate, while a closed-shell structure has been observed for tetracenes (**A4**) connected by four-membered rings (cyclobutadiene moieties) in a linear fashion,[29–31] a radicaloid nature was observed for pentacene (**A5**) units connected by cyclobutadiene moieties in a staggered configuration (Fig. 1).[26] Meanwhile, connecting hexacene units in a three-fold symmetric manner to form starphene resulted in a multi-radical character, with pairs of electrons on each arm.[28]

In this work, we use computation tools to explore the connections between (anti-)aromaticity and multiradical character of molecular materials, which has become increasing important for carbon-based graphenic materials in recent years.[26,28,34–36] The proliferation of acene-based molecules, going beyond their larger counterparts towards dimers,[26,27,30,44] trimers,[28,30,45,46] and other oligomeric derivatives[27,29,31] evidence the rich diversity of materials this family can afford for next-generation molecular magnetic materials. To that aim, we investigate triangular acene derivatives (Fig. 1), generated by combining staggered connections through cyclobutadiene moieties with a three-fold symmetric framework. Using multiconfigurational wavefunction methods, we analyse their electronic structures and, in particular, the mechanisms underlying their predicted open-shell character. This unique architecture, intertwining acene edges with cyclobutadiene linkers, provides an ideal platform to explore how (anti-) aromatic effects interplay with and potentially drive the emergence of multiradical character in these compounds.

Methods

Closed shell singlet (S = 0) structures were first optimized (without geometry constraints) by using the Gaussian16 suite of programs[47] using the restricted Kohn–Sham formalism (RKS) at the M06-2X/6-311+G(d,p) level of theory. The choice of the M06-2X functional is motivated by the need for a high fraction of exact exchange to accurately describe extended conjugated systems such as polyaromatic hydrocarbons. This functional has also been successfully applied to the structural optimization of other conjugated organic compounds with open-shell character.[34,48,49] The stability of S = 0 RKS solutions were checked in all cases. When instabilities were found, the open-shell S = 0 state was further optimized under the unrestricted formalism (UKS) without additional restrictions nor options. Single point calculations and geometry optimization of higher spin states (S = 1, S = 2 and S = 3) were also performed at the UKS level in combination with the same exchange–correlation functional and basis set. Vibrational frequency calculations were routinely performed after each optimization to confirm that optimized structures corresponded to local minima.

Electronic states of different spin multiplicities were further characterized using the restricted active space spin–flip (RAS-SF) approach,[50–53] which has shown excellent performance in the characterization of organic molecules with radical or radicaloid nature.[49,54–58] RAS-SF is based on the splitting of the orbital space into three orbital subspaces: RAS1, RAS2 and RAS3. Then, the RAS-SF wavefunctions of target states are constructed by applying a spin–flip excitation operator to a high-spin reference configuration, typically a Hartree–Fock (HF) state. The excitation operator is typically expanded in all possible excitations within RAS2 ($\hat{r}_0$) and terms progressively including holes in RAS1 (h) and electrons (particles) in RAS3 (p):

$$\hat{R} = \hat{r}_0 + \hat{r}_\mathrm{h} + \hat{r}_\mathrm{p} + \hat{r}_\mathrm{hp} + \hat{r}_\mathrm{2h} + \hat{r}_\mathrm{2p} + \cdots \quad (1)$$

with $\hat{r}_0$ containing all possible excitations within RAS2, and the rest of terms generating configurations with increasing numbers of holes (h subindex) in RAS1, or particles (p subindex) in RAS3. In the present study, we truncate eqn (1) to the first three members, resulting in a rather flexible method with moderate computational cost. RAS-SF energies were obtained in combination with the 6-31G(d,p) basis on the ground state structures optimized at the UKS-M06-2X/6-311+G(d,p) level. The RAS2 space of triangular acenes included 6 electrons in the 6 frontier

π-orbitals in combination with the restricted open-shell HF (ROHF) heptet (S = 3) reference state, while RAS-SF calculations in An molecules were obtained using the lowest ROHF triplet as the reference and with 2 electrons in 2 orbitals RAS2 space. In all calculations, RAS1 and RAS3 subspaces expanded the entire set of doubly occupied and virtual orbitals, respectively. RAS-SF calculations have been carried out with the Q-Chem program.[59]

Results

Molecular structure

Despite the structural constraints imposed by fusing three linear acenes into a triangular framework, all Tn (n = 3–7) molecules adopt planar ground-state geometries. Their optimized structural parameters (*e.g.*, bond lengths) remain largely comparable to those of their linear acene counterparts, with the most pronounced deviations appearing at the edge benzene rings adjacent to the four-membered rings in Tn (Fig. S1). In T3–T7, the four-membered rings display bond lengths characteristic of cyclobutadiene units: the bonds linking the edge acenes exhibit single-bond character (≥1.50 Å), whereas those shared between the four- and six-membered rings are significantly shorter (≤1.40 Å).

Radical character

DFT calculations confirm that the ground states of anthracene (A3), tetracene (A4), pentacene (A5), hexacene (A6), and heptacene (A7) correspond to spin singlets (S = 0), in agreement with previous reports.[22,23] Stability analyses of the RKS solutions further indicate a predominantly closed-shell character across the series, with only A7 exhibiting a mild tendency toward spin-symmetry breaking. In this case, the UKS-optimized geometry is found to be 1.34 kcal mol^{-1} lower in energy than the corresponding RKS solution. The pronounced closed-shell nature of the lower acenes is consistent with extensive evidence in the literature.[16–20,22,23,26,29,55] Triangular acenes also display singlet ground states; however, in contrast to the linear acene series, they exhibit significantly larger UKS-RKS stability differences that increase with molecular size, from 2.3 kcal mol^{-1} in T5 to 7.5 kcal mol^{-1} in T6 and 14.0 kcal mol^{-1} in T7 (Table S1). This trend points to a markedly stronger open-shell character in the larger triangular congeners.

The pronounced open-shell character of the triangular acenes, and its enhancement with increasing molecular size, is further supported by the reduction of their HOMO–LUMO gaps (Table S2, UKS level for those that resulted in instabilities upon stability check, RKS level for those which did not) and by the degree of spin contamination in the UKS ground states, quantified through the expectation value of the S^2 operator (Table S1). A key energetic descriptor closely associated with diradical character is the singlet–triplet energy difference,[2,4,21,23,55]

$$\Delta E(S-T) = E(T) - E(S) \quad (2)$$

Computed singlet–triplet gaps (Tables 1 and S3), evaluated both vertically (at the ground-state geometry) and adiabatically (between the optimized minima of each state), consistently decrease along the An and Tn series, with the triangular acenes displaying markedly smaller values than their linear counterparts. Interestingly, both computational approaches, M06-2X and RAS-SF, yield vertical singlet–triplet gaps in excellent agreement for the An series. In contrast, significantly larger discrepancies arise for the Tn molecules, most likely reflecting the intrinsic limitations of UKS-based methods in accurately capturing systems with pronounced radical character.

Table 1 Calculated vertical singlet–triplet energy gaps (in eV) computed at the M06-2X and RAS-SF levels for the An and Tn series according to eqn (2)

	Linear, An		Triangular, Tn	
n	M06-2X	RAS-SF	M06-2X	RAS-SF
3	2.50	2.50	1.09	1.14
4	1.82	1.95	0.85	0.96
5	1.33	1.45	0.79	0.67
6	0.97	1.11	0.80	0.47
7	0.64	0.72	0.91	0.31

The radical character of the Tn molecules is further corroborated by the analysis of excited states with spin multiplicities beyond the lowest triplet. RAS-SF calculations reveal that the lowest quintet (S = 2) and heptet (S = 3) states of the triangular acenes lie at relatively low energies, particularly for the larger systems, as the singlet–quintet and singlet–heptet gaps decrease with molecular size in a manner similar to the triplet-state energy trend (Fig. 2). These excitation energies are significantly lower than those of the corresponding non-interacting acenes, underscoring the crucial role of inter-acene coupling in shaping the electronic structure of the Tn molecules. Moreover, a dense manifold of spin states is observed below the heptet energy (Fig. S2–S6), consistent with the expected behaviour of three weakly coupled diradicaloid units.

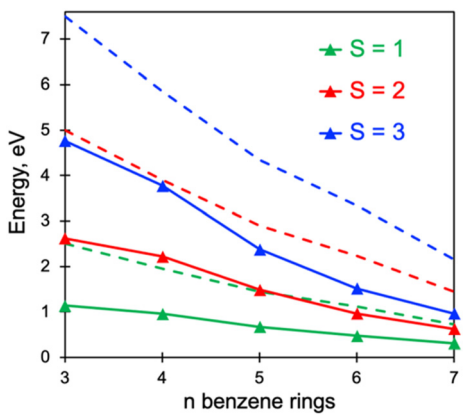

Fig. 2 Energy gaps (in eV) of the lowest triplet (S = 1), quintet (S = 2) and heptet (S = 3) states relative to the ground state singlet of the Tn molecules, computed at the RAS-SF/6-31G(d,p) level. Dashed lines indicate the reference energies of three non-interacting acenes, with quintet and heptet values estimated as twice and three times the triplet energy, respectively.

Alternatively, the radical character of a molecular electronic state can be quantified through the effective number of unpaired electrons. However, because the notion of unpaired electrons is a chemical concept rather than a true physical observable, *i.e.*, no quantum mechanical operator directly defines it, different formulations exist and no single definition is unique. In this work, we adopt the expression introduced by Head-Gordon[60] (eqn (3)), which has been shown to yield more reliable number of unpaired electrons than alternative metrics,[60] applied to the multiconfigurational RAS-SF wavefunctions,

$$N_U = \sum_i \min(n_i, \quad 2 - n_i) \tag{3}$$

where n_i is the electron occupation of the i-th natural orbital ($0 \leq n_i \leq 2$). A N_U value of zero corresponds to a perfect closed-shell structure and increasing values denote stronger radical character.

Table 2 shows the N_U values obtained for the ground state singlet of A*n* and T*n* series. The results are consistent with the singlet–triplet energy differences, once again revealing the pronounced open-shell character of the T*n* series and its progressive increase with molecular size. In general, the N_U values of the T*n* ground states are larger than thrice of the acene counterparts, particularly for the larger members of the series. This is in line with the analysis of S = 1, 2 and 3 energies in Fig. 2, indicating that the radical character of the triangular acenes cannot be attributed solely to the intrinsic diradical nature of the individual acenes (arising from Clar's sextet stabilization); rather, the inter-acene interactions mediated by the cyclobutadiene linkers also contribute significantly to the open-shell character. These findings suggest that an additional mechanism promoting electron unpairing may be operative in the triangular structures.

Aromaticity

Next, we examine the electronic structure of the A*n* and T*n* series through their aromatic and antiaromatic properties, as characterized by the NICS(1) magnetic index, where negative values denote aromaticity, positive values indicate antiaromaticity, and values near zero correspond to nonaromatic character.[61] For the A*n* series, M06-2X calculations at the centres of the six-membered rings reveal local aromaticity, more pronounced in the central rings than at the edges (Fig. S7). The T*n* molecules display a similar pattern across their benzene rings, albeit with systematically reduced aromatic character, as reflected by less negative NICS(1) values (Fig. 3). In contrast, the four-membered rings exhibit strong antiaromatic behaviour, typical of cyclobutadiene,[26,62–64] with markedly positive NICS(1) values. It is worth noting that the antiaromatic character of the cyclobutadiene moieties intensifies with increasing molecular size, whereas the acene fragments in T*n* show a slight enhancement of their aromatic character.

Table 2 Number of unpaired electrons (N_U) for the ground state singlet of A*n* and T*n* molecules computed at the RAS-SF/6-31G(d,p) level

n	A*n*	T*n*
3	0.17	0.41
4	0.15	0.55
5	0.26	1.37
6	0.29	1.85
7	0.48	2.42

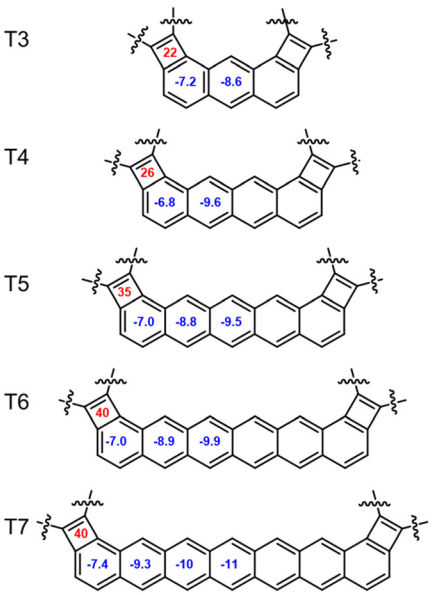

Fig. 3 NICS(1) values M06-2X/6-311++G(2d,p) of the DFT-optimized structures of the T*n*-series. Positive values are denoted in red while negative values are in blue.

Discussion

In the following, we aim to rationalize the results presented in the previous section by providing structural and chemical insights into the enhanced open-shell character of the triangular acenes compared to their linear counterparts.

Structure *vs.* electronic effects

We attribute the differences observed between the A*n* and T*n* series in terms of radical character and aromaticity to two factors: (i) structural distortions imposed by the triangular arrangement and (ii) electronic effects arising from inter-acene couplings. To disentangle these contributions, we examine the properties of linear acenes constrained to the optimized geometries of the T*n* molecules (denoted A*n*′). The comparison between A*n* and A*n*′ isolates the influence of structural distortions while disregarding electronic coupling effects, whereas the comparison between A*n*′ and T*n* highlights the additional role of inter-acene electronic interactions.

Fig. 4a shows the singlet–triplet energy gaps across the A*n*, A*n*′, and T*n* series. The trends clearly indicate that the structural constraints imposed by the triangular framework partially contribute to the reduction of singlet–triplet gaps, as the

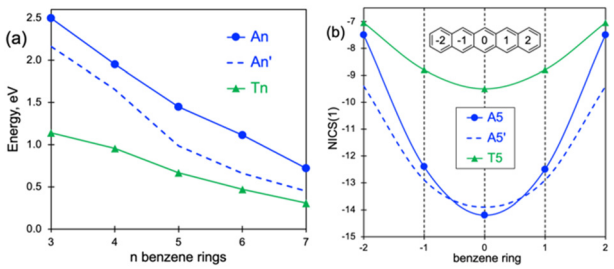

Fig. 4 (a) Singlet–triplet energy gaps (in eV) along the A*n*, A*n*′ and T*n* series computed at the RAS-SF/6-31G(d,p) level. (b) NICS(1) values at the center of the six-member rings in A5, A5′ and T5 molecules computed at the M06-2X/6-311+G(d,p) level.

A*n*′ values consistently fall between those of A*n* and T*n*. Furthermore, the results suggest that electronic coupling effects dominate in the smaller triangular systems (T3 and T4), whereas in the larger members (T5, T6, and T7) structural distortions play a comparatively greater role in lowering the singlet–triplet gaps.

Structural constraints also make a non-negligible contribution to the local aromaticities of the benzene rings. Fig. 4b compares the NICS(1) values at the centers of the benzene rings in A5, A5′, and T5, with analogous plots for the remaining systems provided in the SI (Fig. S8). The NICS(1) profile of A5′ closely parallels that of T5, though shifted toward more negative values, similar to A5. Analysis of the NICS(1) values for the other systems indicates that the relative importance of structural effects is weaker in the smaller molecules (T3 and T4), consistent with the trends observed for the singlet–triplet energy gaps. Overall, these results suggest that the reduction of local aromaticity in the triangular systems is primarily driven by electronic effects rather than structural distortions.

Electronic mechanism

Next, we further analyze the electronic effects underlying the differences between A*n* and T*n*. Beyond the mere increase in the number of six-membered rings, the connectivity through cyclobutadiene moieties appears to promote the (multi)radical nature of these molecules. The mechanisms underlying the emergence of unpaired electrons in T*n* can be schematically illustrated through their most stable resonance structures (Fig. 5). For instance, T5-II corresponds to a resonance form analogous to the well-known sextet migration in linear acenes, which preserves the balance between aromatic sextets and anti-aromatic cyclobutadiene units. From this structure, one can generate additional resonance forms bearing two unpaired electrons on each acene arm. These can be classified into two families: (i) forms with unpaired electrons delocalized onto the four-membered rings (T5-III in Fig. 5); and (ii) forms with unpaired electrons localized at the zigzag edges of the acene fragments (T5-IV in Fig. 5), directly related to the intrinsic diradicaloid character of linear acenes. In both, breaking double bonds on the four-membered rings relieve the Hückel antiaromatic character of the cyclobutadiene moieties, while the latter (T5-IV) is stabilized further by the formation of additional Clar's sextets.[26]

We note that the breaking of the cyclobutadiene moiety to a radialene moiety has been observed experimentally in acene dimers connected by four-membered rings,[65] while the decrease in anti-aromatic character of cyclobutadiene moieties in favor of a diradical character is consistent with a previous result on pentacene dimers.[26] The coexistence of the diradical resonance forms III and IV in the ground state of T*n* molecules suggests that their radical character arises from the interplay of two complementary mechanisms: Clar's sextet stabilization and the relief of antiaromaticity. To illustrate this, we analyze the spatial distribution of the unpaired electron density using the fractional occupation density (FOD) method,[66,67] introduced by Hansen and Grimme, defined as:

$$\rho^{\mathrm{FOD}}(r) = \sum_i \min(n_i, \quad 2 - n_i)\phi_i^*(r)\phi_i(r) \qquad (4)$$

where ϕ_i is the natural orbital with electron occupation n_i. Notice that the integration of the FOD corresponds to N_U (eqn (3)).

Fig. 6 shows the FODs of the ground-state singlet for the T*n* series computed at the RAS-SF/6-31G(d,p) level. In T3, the unpaired electron density is largely localized on the four-membered ring carbons, consistent with resonance forms that alleviate antiaromaticity, with only minor contributions from the

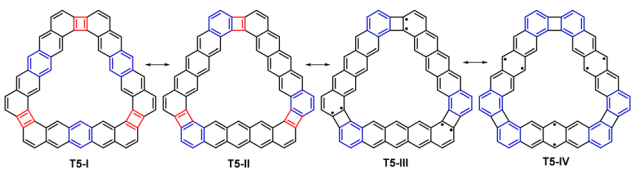

Fig. 5 Resonance structures for T5 molecule, with aromatic Clar's sextets indicated in blue and antiaromatic cyclobutadiene units in red.

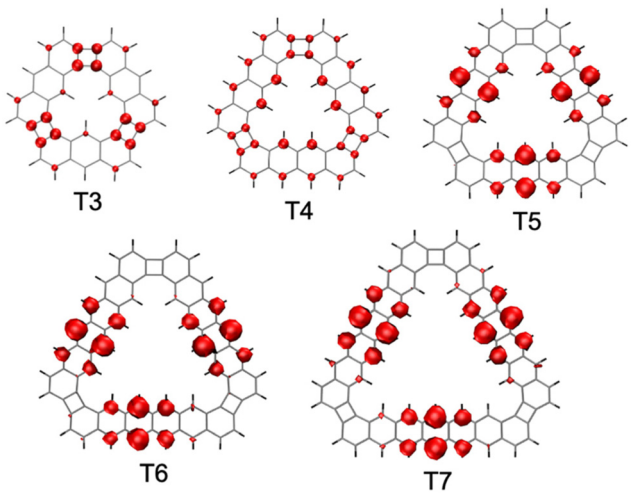

Fig. 6 Representation of the ground state singlet FOD of T*n* molecules computed at the RAS-SF/6-31G(d,p) level. Isovalue = 0.001 au.

other carbon atoms, schematically corresponding to resonance structure III in Fig. 5. In T4, the unpaired electrons remain delocalized over the four-membered rings, but also extend along the acenes, indicating the simultaneous involvement of both resonance forms in the ground-state electronic structure. For the larger T*n* molecules (T5–T7), however, the unpaired electron density is predominantly distributed over the zigzag carbons at the center of the acenes, in agreement with Clar's sextet stabilization, and corresponding to resonance structure IV in Fig. 5. These contrasting distributions rationalize the distinct origins of radical character across the series: in smaller molecules, the decrease in cyclobutadiene antiaromaticity dominates, whereas in T5–T7 the radical character is primarily associated with central acene delocalization, leading to a nearly constant level of antiaromaticity release. This trend also aligns with the singlet–triplet energy behavior, where electron coupling through the inter-acene connections plays a major role in T3 and T4, but becomes progressively weaker as the number of benzene rings increases and the unpaired electrons localize within the acenes.

Conclusions

We have explored the electronic structure of triangular acenes (T*n*, n = 3–7) in comparison with linear acenes (A*n*), combining density functional and multiconfigurational approaches. Triangular acenes exhibit a markedly stronger radical character, which arises from the interplay between Clar's sextet stabilization and the release of cyclobutadiene antiaromaticity. Spin-state energetics, unpaired electron densities, and NICS(1) aromaticity indices consistently reveal that T*n* molecules display reduced singlet–triplet gaps, stronger multiradical character, and a distinctive redistribution of unpaired electrons with increasing size. Structural restrictions imposed by triangular connectivity contribute to these trends, though inter-acene couplings play the dominant role in smaller members. Overall, triangular acenes emerge as a new class of acene derivatives where topology dictates radical character and aromaticity, providing valuable insights for the design of open-shell π-conjugated systems and novel carbon-based materials.

Author contributions

All authors contributed to the conceptualization and design of the study, carried out the calculations, analyzed the results, and were involved in manuscript preparation. J. P. C. and D. C. provided supervision.

Conflicts of interest

There are no conflicts to declare.

Data availability

The data supporting this article have been included as part of the supplementary information (SI). Supplementary information is available. See DOI: **https://doi.org/10.1039/d5qo01343g**.

Acknowledgements

We acknowledge financial support from MCIU/AEI/10.13039/501100011033 (projects PID2022-136231NB-I00 and RED2024-154178-T). The authors are thankful for the technical and human support provided by the Donostia International Physics Center (DIPC) Computer Center. D. C. is thankful for financial support from IKERBASQUE (Basque Foundation for Science). J. P. C. acknowledges the access granted to the HPC resources of the SACADO MeSU platform at Sorbonne Université and the Marie Skłodowska-Curie Actions Postdoctoral Fellowship (Grant Agreement No. 101153230).

References

1 M. Abe, Diradicals, *Chem. Rev.*, 2013, **113**, 7011–7088.
2 T. Stuyver, B. Chen, T. Zeng, P. Geerlings, F. De Proft and R. Hoffmann, Do Diradicals Behave Like Radicals?, *Chem. Rev.*, 2019, **119**, 11291–11351.
3 A. Hinz, J. Bresien, F. Breher and A. Schulz, Heteroatom-Based Diradical(oid)s, *Chem. Rev.*, 2023, **123**, 10468–10526.
4 A. Mizuno, R. Matsuoka, T. Mibu and T. Kusamoto, Luminescent Radicals, *Chem. Rev.*, 2024, **124**, 1034–1121.
5 P. Murto and H. Bronstein, Electro-optical π-radicals: design advances, applications and future perspectives, *J. Mater. Chem. C*, 2022, **10**, 7368–7403.
6 K. Hatakeyama-Sato and K. Oyaizu, Redox: Organic Robust Radicals and Their Polymers for Energy Conversion/Storage Devices, *Chem. Rev.*, 2023, **123**, 11336–11391.
7 H. Yeo, S. Debnath, B. P. Krishnan and B. W. Boudouris, Radical polymers in optoelectronic and spintronic applications, *RSC Appl. Polym.*, 2024, **2**, 7–25.
8 Y. Tan, S.-N. Hsu, H. Tahir, L. Dou, B. M. Savoie and B. W. Boudouris, Electronic and Spintronic Open-Shell Macromolecules, *Quo Vadis ?*, *J. Am. Chem. Soc.*, 2022, **144**, 626–647.
9 Y. Sumida and H. Ohmiya, Direct excitation strategy for radical generation in organic synthesis, *Chem. Soc. Rev.*, 2021, **50**, 6320–6332.
10 D. Leifert and A. Studer, Organic Synthesis Using Nitroxides, *Chem. Rev.*, 2023, **123**, 10302–10380.
11 G. J. Rowlands, Radicals in organic synthesis. Part 1, *Tetrahedron*, 2009, **65**, 8603–8655.
12 Z. X. Chen, Y. Li and F. Huang, Persistent and Stable Organic Radicals: Design, Synthesis, and Applications, *Chem*, 2021, **7**, 288–332.

13 K. Kato and A. Osuka, Platforms for Stable Carbon–Centered Radicals, *Angew. Chem., Int. Ed.*, 2019, **58**, 8978–8986.
14 D. G. de Oteyza and T. Frederiksen, Carbon-based nanostructures as a versatile platform for tunable π-magnetism, *J. Phys.: Condens. Matter*, 2022, **34**, 443001.
15 S. Song, J. Su, M. Telychko, J. Li, G. Li, Y. Li, C. Su, J. Wu and J. Lu, On-surface synthesis of graphene nanostructures with π-magnetism, *Chem. Soc. Rev.*, 2021, **50**, 3238–3262.
16 C. Tönshoff and H. F. Bettinger, Pushing the Limits of Acene Chemistry: The Recent Surge of Large Acenes, *Chem. – Eur. J.*, 2021, **27**, 3193–3212.
17 H. Hayashi and H. Yamada, Exploring the chemistry of higher acenes: from synthesis to applications, *Chem. Sci.*, 2025, **16**, 11204–11231.
18 H. Yamada and H. Hayashi, Synthesis of oligoacenes using precursors for evaluation of their electronic structures, *Photochem. Photobiol. Sci.*, 2022, **21**, 1511–1532.
19 J. E. Anthony, Functionalized Acenes and Heteroacenes for Organic Electronics, *Chem. Rev.*, 2006, **106**, 5028–5048.
20 P. M. Greißel, A.-S. Wollny, Y. Bo, D. Thiel, R. Weiß and D. M. Guldi, Molecular Acenes for Light Capture, Conversion, and Storage, *Acc. Mater. Res.*, 2025, **6**, 172–182.
21 D. Jiang and S. Dai, Electronic Ground State of Higher Acenes, *J. Phys. Chem. A*, 2008, **112**, 332–335.
22 M. Bendikov, H. M. Duong, K. Starkey, K. N. Houk, E. A. Carter and F. Wudl, Oligoacenes: Theoretical Prediction of Open-Shell Singlet Diradical Ground States, *J. Am. Chem. Soc.*, 2004, **126**, 7416–7417.
23 C.-N. Yeh and J.-D. Chai, Role of Kekulé and Non-Kekulé Structures in the Radical Character of Alternant Polycyclic Aromatic Hydrocarbons: A TAO-DFT Study, *Sci. Rep.*, 2016, **6**, 30562.
24 D. Khan, A. J. A. Price, B. Huang, M. L. Ach and O. A. Von Lilienfeld, Adapting hybrid density functionals with machine learning, *Sci. Adv.*, 2025, **11**, eadt7769.
25 R. Zuzak, M. Kumar, O. Stoica, D. Soler-Polo, J. Brabec, K. Pernal, L. Veis, R. Blieck, A. M. Echavarren, P. Jelinek and S. Godlewski, On–Surface Synthesis and Determination of the Open–Shell Singlet Ground State of Tridecacene**, *Angew. Chem., Int. Ed.*, 2024, **63**, e202317091.
26 T. Wang, P. Angulo-Portugal, A. Berdonces-Layunta, A. Jancarik, A. Gourdon, J. Holec, M. Kumar, D. Soler, P. Jelinek, D. Casanova, M. Corso, D. G. De Oteyza and J. P. Calupitan, Tuning the Diradical Character of Pentacene Derivatives via Non-Benzenoid Coupling Motifs, *J. Am. Chem. Soc.*, 2023, **145**, 10333–10341.
27 P. Cui, Q. Zhang, H. Zhu, X. Li, W. Wang, Q. Li, C. Zeng and Z. Zhang, Carbon Tetragons as Definitive Spin Switches in Narrow Zigzag Graphene Nanoribbons, *Phys. Rev. Lett.*, 2016, **116**, 026802.
28 J. Besteiro-Sáez, L. M. Mateo, S. Salaverría, T. Wang, P. Angulo-Portugal, J. P. Calupitan, J. Rodríguez-Fernández, A. García-Fuente, J. Ferrer, D. Pérez, M. Corso, D. G. De Oteyza and D. Peña, [19]Starphene: Combined In–Solution and On–Surface Synthesis Towards the Largest Starphene, *Angew. Chem., Int. Ed.*, 2024, **63**, e202411861.
29 C. Sánchez-Sánchez, T. Dienel, A. Nicolaï, N. Kharche, L. Liang, C. Daniels, V. Meunier, J. Liu, X. Feng, K. Müllen, J. R. Sánchez-Valencia, O. Gröning, P. Ruffieux and R. Fasel, On–Surface Synthesis and Characterization of Acene–Based Nanoribbons Incorporating Four–Membered Rings, *Chem. – Eur. J.*, 2019, **25**, 12074–12082.
30 M. Koch, M. Gille, S. Hecht and L. Grill, Steering a cycloaddition reaction via the surface structure, *Surf. Sci.*, 2018, **678**, 194–200.
31 C. Sánchez-Sánchez, A. Nicolaï, F. Rossel, J. Cai, J. Liu, X. Feng, K. Müllen, P. Ruffieux, R. Fasel and V. Meunier, On-Surface Cyclization of *ortho* -Dihalotetracenes to Four- and Six-Membered Rings, *J. Am. Chem. Soc.*, 2017, **139**, 17617–17623.
32 E. Turco, A. Bernhardt, N. Krane, L. Valenta, R. Fasel, M. Juríček and P. Ruffieux, Observation of the Magnetic Ground State of the Two Smallest Triangular Nanographenes, *JACS Au*, 2023, **3**, 1358–1364.
33 N. Pavliček, A. Mistry, Z. Majzik, N. Moll, G. Meyer, D. J. Fox and L. Gross, Synthesis and characterization of triangulene, *Nat. Nanotechnol.*, 2017, **12**, 308–311.
34 T. Wang, A. Berdonces-Layunta, N. Friedrich, M. Vilas-Varela, J. P. Calupitan, J. I. Pascual, D. Peña, D. Casanova, M. Corso and D. G. de Oteyza, Aza-Triangulene: On-Surface Synthesis and Electronic and Magnetic Properties, *J. Am. Chem. Soc.*, 2022, **144**, 4522–4529.
35 J. P. Calupitan, A. Berdonces-Layunta, F. Aguilar-Galindo, M. Vilas-Varela, D. Peña, D. Casanova, M. Corso, D. G. De Oteyza and T. Wang, Emergence of π-Magnetism in Fused Aza-Triangulenes: Symmetry and Charge Transfer Effects, *Nano Lett.*, 2023, **23**, 9832–9840.
36 M. Vilas-Varela, F. Romero-Lara, A. Vegliante, J. P. Calupitan, A. Martínez, L. Meyer, U. Uriarte-Amiano, N. Friedrich, D. Wang, F. Schulz, N. E. Koval, M. E. Sandoval-Salinas, D. Casanova, M. Corso, E. Artacho, D. Peña and J. I. Pascual, On–Surface Synthesis and Characterization of a High–Spin Aza–[5]–Triangulene, *Angew. Chem., Int. Ed.*, 2023, **62**, e202307884.
37 S. Arikawa, A. Shimizu, D. Shiomi, K. Sato, T. Takui, H. Sotome, H. Miyasaka, M. Murai, S. Yamaguchi and R. Shintani, A Kinetically Stabilized Nitrogen–Doped Triangulene Cation: Stable and NIR Fluorescent Diradical Cation with Triplet Ground State, *Angew. Chem.*, 2023, e202302714.
38 S. Arikawa, A. Shimizu, D. Shiomi, K. Sato and R. Shintani, Synthesis and Isolation of a Kinetically Stabilized Crystalline Triangulene, *J. Am. Chem. Soc.*, 2021, **143**, 19599–19605.
39 L. Valenta, M. Mayländer, P. Kappeler, O. Blacque, T. Šolomek, S. Richert and M. Juríček, Trimesityltriangulene: a persistent derivative of Clar's hydrocarbon, *Chem. Commun.*, 2022, **58**, 3019–3022.
40 T. Jiao, C.-H. Wu, Y.-S. Zhang, X. Miao, S. Wu, S.-D. Jiang and J. Wu, Solution-phase synthesis of Clar's goblet and

elucidation of its spin properties, *Nat. Chem.*, 2025, **17**, 924–932.

41 S. Mishra, D. Beyer, K. Eimre, S. Kezilebieke, R. Berger, O. Gröning, C. A. Pignedoli, K. Müllen, P. Liljeroth, P. Ruffieux, X. Feng and R. Fasel, Topological frustration induces unconventional magnetism in a nanographene, *Nat. Nanotechnol.*, 2020, **15**, 22–28.

42 S. Mishra, M. Vilas-Varela, I. Rončević, F. Paschke, F. Albrecht, L. Gross and D. Peña, Synthesis and Characterization of a π-Extended Clar's Goblet, *J. Am. Chem. Soc.*, 2025, **147**, 39067–39071.

43 M. Bursch, J. Mewes, A. Hansen and S. Grimme, Best–Practice DFT Protocols for Basic Molecular Computational Chemistry**, *Angew. Chem.*, 2022, **134**, e202205735.

44 I. Izydorczyk, O. Stoica, M. Krawiec, R. Blieck, R. Zuzak, M. Stępień, A. M. Echavarren and S. Godlewski, On-surface synthesis of a phenylene analogue of nonacene, *Chem. Commun.*, 2022, **58**, 4063–4066.

45 M. S. G. Mohammed, J. Lawrence, F. García, P. Brandimarte, A. Berdonces-Layunta, D. Pérez, D. Sánchez-Portal, D. Peña and D. G. de Oteyza, From starphenes to non-benzenoid linear conjugated polymers by substrate templating, *Nanoscale Adv.*, 2021, **3**, 2351–2358.

46 J. Holec, B. Cogliati, J. Lawrence, A. Berdonces-Layunta, P. Herrero, Y. Nagata, M. Banasiewicz, B. Kozankiewicz, M. Corso, D. G. De Oteyza, A. Jancarik and A. Gourdon, A Large Starphene Comprising Pentacene Branches, *Angew. Chem., Int. Ed.*, 2021, **60**, 7752–7758.

47 M. J. Frisch, G. W. Trucks, H. B. Schlegel, G. E. Scuseria, M. A. Robb, J. R. Cheeseman, G. Scalmani, V. Barone, G. A. Petersson, H. Nakatsuji, X. Li, M. Caricato, A. V. Marenich, J. Bloino, B. G. Janesko, R. Gomperts, B. Mennucci, H. P. Hratchian, J. V. Ortiz, A. F. Izmaylov, J. L. Sonnenberg, D. Williams-Young, F. Ding, F. Lipparini, F. Egidi, J. Goings, B. Peng, A. Petrone, T. Henderson, D. Ranasinghe, V. G. Zakrzewski, J. Gao, N. Rega, G. Zheng, W. Liang, M. Hada, M. Ehara, K. Toyota, R. Fukuda, J. Hasegawa, M. Ishida, T. Nakajima, Y. Honda, O. Kitao, H. Nakai, T. Vreven, K. Throssell, J. A. Montgomery Jr., J. E. Peralta, F. Ogliaro, M. J. Bearpark, J. J. Heyd, E. N. Brothers, K. N. Kudin, V. N. Staroverov, T. A. Keith, R. Kobayashi, J. Normand, K. Raghavachari, A. P. Rendell, J. C. Burant, S. S. Iyengar, J. Tomasi, M. Cossi, J. M. Millam, M. Klene, C. Adamo, R. Cammi, J. W. Ochterski, R. L. Martin, K. Morokuma, O. Farkas, J. B. Foresman and D. J. Fox, *Gaussian 16, Revision C.01*, 2016.

48 E. San-Fabián, A. Pérez-Guardiola, M. Moral, A. J. Pérez-Jiménez and J. C. Sancho-García, in *Advanced Magnetic and Optical Materials*, ed. A. Tiwari, P. K. Iyer, V. Kumar and H. Swart, Wiley, 1st edn, 2016, pp. 165–183.

49 M. E. Sandoval-Salinas, A. Carreras and D. Casanova, Triangular graphene nanofragments: open-shell character and doping, *Phys. Chem. Chem. Phys.*, 2019, **21**, 9069–9076.

50 D. Casanova, Efficient implementation of restricted active space configuration interaction with the hole and particle approximation, *J. Comput. Chem.*, 2013, **34**, 720–730.

51 D. Casanova, Avoided crossings, conical intersections, and low-lying excited states with a single reference method: The restricted active space spin-flip configuration interaction approach, *J. Chem. Phys.*, 2012, **137**, 084105.

52 D. Casanova, Restricted active space configuration interaction methods for strong correlation: Recent developments, *Wiley Interdiscip. Rev.:Comput. Mol. Sci.*, 2022, **12**, e1561.

53 D. Casanova and M. Head-Gordon, Restricted active space spin-flip configuration interaction approach: theory, implementation and examples, *Phys. Chem. Chem. Phys.*, 2009, **11**, 9779.

54 M. Desroches, P. Mayorga-Burrezo, J. Boismenu-Lavoie, M. Peña Álvarez, C. J. Gómez-García, J. M. Matxain, D. Casanova, J. Morin and J. Casado, Breaking Bonds and Forming Nanographene Diradicals with Pressure, *Angew. Chem., Int. Ed.*, 2017, **56**, 16212–16217.

55 A. Pérez-Guardiola, M. E. Sandoval-Salinas, D. Casanova, E. San-Fabián, A. J. Pérez-Jiménez and J. C. Sancho-García, The role of topology in organic molecules: origin and comparison of the radical character in linear and cyclic oligoacenes and related oligomers, *Phys. Chem. Chem. Phys.*, 2018, **20**, 7112–7124.

56 Z. Li, T. Y. Gopalakrishna, Y. Han, Y. Gu, L. Yuan, W. Zeng, D. Casanova and J. Wu, [6]Cyclo- *para* -phenylmethine: An Analog of Benzene Showing Global Aromaticity and Open-Shell Diradical Character, *J. Am. Chem. Soc.*, 2019, **141**, 16266–16270.

57 C. Liu, M. E. Sandoval-Salinas, Y. Hong, T. Y. Gopalakrishna, H. Phan, N. Aratani, T. S. Herng, J. Ding, H. Yamada, D. Kim, D. Casanova and J. Wu, Macrocyclic Polyradicaloids with Unusual Super-ring Structure and Global Aromaticity, *Chem*, 2018, **4**, 1586–1595.

58 J. A. Rodríguez-Jiménez, A. Carreras and D. Casanova, Spin–Orbit Couplings of Open-Shell Systems with Restricted Active Space Configuration Interaction, *J. Phys. Chem. A*, 2023, **127**, 1206–1218.

59 E. Epifanovsky, A. T. B. Gilbert, X. Feng, J. Lee, Y. Mao, N. Mardirossian, P. Pokhilko, A. F. White, M. P. Coons, A. L. Dempwolff, Z. Gan, D. Hait, P. R. Horn, L. D. Jacobson, I. Kaliman, J. Kussmann, A. W. Lange, K. U. Lao, D. S. Levine, J. Liu, S. C. McKenzie, A. F. Morrison, K. D. Nanda, F. Plasser, D. R. Rehn, M. L. Vidal, Z.-Q. You, Y. Zhu, B. Alam, B. J. Albrecht, A. Aldossary, E. Alguire, J. H. Andersen, V. Athavale, D. Barton, K. Begam, A. Behn, N. Bellonzi, Y. A. Bernard, E. J. Berquist, H. G. A. Burton, A. Carreras, K. Carter-Fenk, R. Chakraborty, A. D. Chien, K. D. Closser, V. Cofer-Shabica, S. Dasgupta, M. De Wergifosse, J. Deng, M. Diedenhofen, H. Do, S. Ehlert, P.-T. Fang, S. Fatehi, Q. Feng, T. Friedhoff, J. Gayvert, Q. Ge, G. Gidofalvi, M. Goldey, J. Gomes, C. E. González-Espinoza, S. Gulania, A. O. Gunina, M. W. D. Hanson-Heine, P. H. P. Harbach, A. Hauser, M. F. Herbst, M. Hernández Vera, M. Hodecker, Z. C. Holden, S. Houck, X. Huang, K. Hui, B. C. Huynh, M. Ivanov, Á. Jász, H. Ji, H. Jiang,

B. Kaduk, S. Kähler, K. Khistyaev, J. Kim, G. Kis, P. Klunzinger, Z. Koczor-Benda, J. H. Koh, D. Kosenkov, L. Koulias, T. Kowalczyk, C. M. Krauter, K. Kue, A. Kunitsa, T. Kus, I. Ladjánszki, A. Landau, K. V. Lawler, D. Lefrancois, S. Lehtola, R. R. Li, Y.-P. Li, J. Liang, M. Liebenthal, H.-H. Lin, Y.-S. Lin, F. Liu, K.-Y. Liu, M. Loipersberger, A. Luenser, A. Manjanath, P. Manohar, E. Mansoor, S. F. Manzer, S.-P. Mao, A. V. Marenich, T. Markovich, S. Mason, S. A. Maurer, P. F. McLaughlin, M. F. S. J. Menger, J.-M. Mewes, S. A. Mewes, P. Morgante, J. W. Mullinax, K. J. Oosterbaan, G. Paran, A. C. Paul, S. K. Paul, F. Pavošević, Z. Pei, S. Prager, E. I. Proynov, Á. Rák, E. Ramos-Cordoba, B. Rana, A. E. Rask, A. Rettig, R. M. Richard, F. Rob, E. Rossomme, T. Scheele, M. Scheurer, M. Schneider, N. Sergueev, S. M. Sharada, W. Skomorowski, D. W. Small, C. J. Stein, Y.-C. Su, E. J. Sundstrom, Z. Tao, J. Thirman, G. J. Tornai, T. Tsuchimochi, N. M. Tubman, S. P. Veccham, O. Vydrov, J. Wenzel, J. Witte, A. Yamada, K. Yao, S. Yeganeh, S. R. Yost, A. Zech, I. Y. Zhang, X. Zhang, Y. Zhang, D. Zuev, A. Aspuru-Guzik, A. T. Bell, N. A. Besley, K. B. Bravaya, B. R. Brooks, D. Casanova, J.-D. Chai, S. Coriani, C. J. Cramer, G. Cserey, A. E. DePrince, R. A. DiStasio, A. Dreuw, B. D. Dunietz, T. R. Furlani, W. A. Goddard, S. Hammes-Schiffer, T. Head-Gordon, W. J. Hehre, C.-P. Hsu, T.-C. Jagau, Y. Jung, A. Klamt, J. Kong, D. S. Lambrecht, W. Liang, N. J. Mayhall, C. W. McCurdy, J. B. Neaton, C. Ochsenfeld, J. A. Parkhill, R. Peverati, V. A. Rassolov, Y. Shao, L. V. Slipchenko, T. Stauch, R. P. Steele, J. E. Subotnik, A. J. W. Thom, A. Tkatchenko, D. G. Truhlar, T. Van Voorhis, T. A. Wesolowski, K. B. Whaley, H. L. Woodcock, P. M. Zimmerman, S. Faraji, P. M. W. Gill, M. Head-Gordon, J. M. Herbert and A. I. Krylov, Software for the frontiers of quantum chemistry: An overview of developments in the Q-Chem 5 package, *J. Chem. Phys.*, 2021, **155**, 084801.

60 M. Head-Gordon, Characterizing unpaired electrons from the one-particle density matrix, *Chem. Phys. Lett.*, 2003, **372**, 508–511.

61 P. V. R. Schleyer, C. Maerker, A. Dransfeld, H. Jiao and N. J. R. van Eikema Hommes, Nucleus-Independent Chemical Shifts: A Simple and Efficient Aromaticity Probe, *J. Am. Chem. Soc.*, 1996, **118**, 6317–6318.

62 P. H. Jacobse, Z. Jin, J. Jiang, S. Peurifoy, Z. Yue, Z. Wang, D. J. Rizzo, S. G. Louie, C. Nuckolls and M. F. Crommie, Pseudo-atomic orbital behavior in graphene nanoribbons with four-membered rings, *Sci. Adv.*, 2021, **7**, eabl5892.

63 Z. Jin, Y. C. Teo, S. J. Teat and Y. Xia, Regioselective Synthesis of [3]Naphthylenes and Tuning of Their Antiaromaticity, *J. Am. Chem. Soc.*, 2017, **139**, 15933–15939.

64 Y. C. Teo, Z. Jin and Y. Xia, Synthesis of Cyclobutadienoid-Fused Phenazines with Strongly Modulated Degrees of Antiaromaticity, *Org. Lett.*, 2018, **20**, 3300–3304.

65 S. Kawai, K. Takahashi, S. Ito, R. Pawlak, T. Meier, P. Spijker, F. F. Canova, J. Tracey, K. Nozaki, A. S. Foster and E. Meyer, Competing Annulene and Radialene Structures in a Single Anti-Aromatic Molecule Studied by High-Resolution Atomic Force Microscopy, *ACS Nano*, 2017, **11**, 8122–8130.

66 S. Grimme and A. Hansen, A Practicable Real–Space Measure and Visualization of Static Electron–Correlation Effects, *Angew. Chem., Int. Ed.*, 2015, **54**, 12308–12313.

67 C. A. Bauer, A. Hansen and S. Grimme, The Fractional Occupation Number Weighted Density as a Versatile Analysis Tool for Molecules with a Complicated Electronic Structure, *Chem. – Eur. J.*, 2017, **23**, 6150–6164.

